



## Assessment of Rainwater Harvesting Quantity and Treatment Quality Using Combined Silica Sand-Activated Carbon-Membrane Filtration in Sungai Langka Village, Indonesia

Pritama Fauziyah<sup>1,2</sup>, Nabila Evqi Putri<sup>1,2</sup>, Andika Munandar<sup>1</sup>, Indah Yusliga Sari Purba<sup>1</sup>, Tarmizi Taher<sup>1,2</sup>,  

<sup>1</sup>Department of Environmental Engineering, Faculty of Infrastructure and Regional Technology, Institut Teknologi Sumatera, Lampung Selatan 35365, Indonesia

<sup>2</sup>Center for Green and Sustainable Materials, Institut Teknologi Sumatera, Lampung Selatan 35365, Indonesia

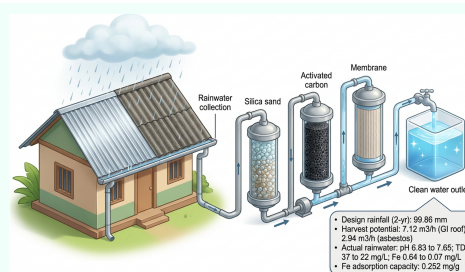
✉ Corresponding author: tarmizi.taher@itera.ac.id

 **ARTICLE HISTORY:**  Received: January 15, 2026 |  Revised: January 28, 2026 |  Accepted: February 5, 2026

### ABSTRACT

Clean water scarcity remains a critical challenge in many regions of Indonesia, particularly in rural areas such as Sungai Langka Village, Pesawaran Regency, Lampung Province. This study investigates rainwater harvesting (RWH) as an alternative clean water source by developing a combined filtration-adsorption treatment system consisting of three sequential columns—silica sand, activated carbon, and filter membrane—operated in continuous-flow mode. The research objectives include determining rainwater harvesting potential, optimizing the treatment system through artificial water testing, and evaluating treated rainwater quality against regulatory standards. Analysis of rainfall data from 2015–2024 using the Gumbel distribution method yielded a 2-year return period design rainfall of 99.86 mm, corresponding to harvesting potentials of 7.12 m<sup>3</sup>/hour and 2.94 m<sup>3</sup>/hour for galvanized iron and asbestos roofs, respectively. System optimization with artificial water demonstrated effective contaminant removal under extreme conditions, achieving up to 62.54% TDS removal and 82.19% Fe removal. Treatment of actual rainwater successfully adjusted pH from 6.83 to 7.65, reduced TDS from 37 to 22 mg/L (40.54%), and decreased Fe concentration from 0.64 to 0.07 mg/L (89.06%), with an Fe adsorption capacity of 0.252 mg/g. All treated water parameters met the Indonesian Minister of Health Regulation No. 2/2023 standards for sanitary hygiene water, confirming the system as a practical and affordable point-of-use solution for improving clean water access in water-scarce rural communities.

**Keywords:** rainwater harvesting; filtration; adsorption; water quality; silica sand; activated carbon



### 1. Introduction

CLEAN water scarcity represents one of the most pressing challenges facing many regions in Indonesia [1]. Sungai Langka Village in Pesawaran Regency, Lampung Province, experiences limited water availability due to increasing groundwater extraction from agricultural, industrial, and domestic sectors, compounded by global climate change. Rainwater harvesting (RWH) offers a promising alternative for clean water provision, particularly during the rainy season when surface runoff exceeds soil infiltration capacity [2, 3].

Rainwater harvesting is defined as the collection and storage of rainwater for subsequent use during periods of low precipitation [4]. This technique can be implemented through rooftop collection systems or surface runoff reservoirs, with rooftop systems being more suitable for household and community-scale applications due to their relatively cleaner catchment surfaces and simpler infrastructure requirements. The Indonesian Ministry of Environment Regulation No. 12/2009 encourages the development of RWH systems across various regions to promote sustainable water management and reduce dependency on groundwater extraction. However, field implementation remains limited, particularly in rural areas, due to inadequate technical knowledge, lack of affordable treatment technologies, and insufficient under-

standing of local rainwater quality characteristics [1].

The utilization of harvested rainwater requires specific treatment to meet clean water quality standards as stipulated in the Indonesian Minister of Health Regulation No. 2/2023 concerning Sanitary Hygiene Water [5]. Rainwater characteristics depend on geographical location, atmospheric conditions, and surrounding pollution factors [6]. In tropical regions such as Indonesia, rainwater is generally acidic (pH 5–6.5) due to the dissolution of atmospheric CO<sub>2</sub> forming carbonic acid (H<sub>2</sub>CO<sub>3</sub>), as well as sulfur dioxide (SO<sub>2</sub>) and nitrogen oxides (NO<sub>x</sub>) from vehicular emissions and industrial activities that form sulfuric and nitric acids [7]. Collected rainwater typically contains suspended particulate matter including dust, leaves, bird droppings, and atmospheric aerosols that accumulate on rooftop surfaces during dry periods and are washed off during the first flush of rainfall events [8, 9].

Rooftop rainwater quality is further compromised by leaching of materials from roofing surfaces. Galvanized iron roofs, commonly used in rural Indonesia, release zinc (Zn) and iron (Fe) through corrosion processes, with Fe concentrations often exceeding the regulatory limit of 0.3 mg/L [10–12]. Asbestos and clay tile roofs contribute silicates and calcium compounds that elevate total dissolved solids (TDS). Additionally, organic matter from decomposing vegetation and microbial biofilms on roof surfaces introduces dissolved

organic carbon and pathogenic microorganisms into the harvested water [6]. These multiple contamination pathways necessitate multi-barrier treatment approaches to ensure water safety.

Several methods can be employed for rainwater treatment, including chemical coagulation-flocculation, chlorination, ultraviolet (UV) disinfection, membrane filtration, and adsorption [5]. Among physical treatment methods, filtration is commonly used as a preliminary stage to remove suspended particles through mechanical straining and depth filtration mechanisms [13]. Silica sand filtration, in particular, provides dual functions: physical removal of particles larger than the pore size (typically 10–100  $\mu\text{m}$ ) and surface adsorption of fine colloids onto negatively charged silanol (Si–OH) groups [14]. However, filtration alone is insufficient to remove dissolved ionic species such as heavy metals ( $\text{Fe}^{2+}$ ,  $\text{Fe}^{3+}$ ,  $\text{Zn}^{2+}$ ), acidic compounds, and dissolved organic matter that remain in the aqueous phase after passing through the filter bed.

Adsorption has emerged as a complementary and essential step for removing dissolved contaminants from water [15, 16]. Activated carbon, characterized by its highly developed microporous structure (surface areas of 500–1500  $\text{m}^2/\text{g}$ ) and oxygen-containing surface functional groups (carboxyl, hydroxyl, carbonyl, phenolic), exhibits strong affinity for adsorbing heavy metal cations through ion exchange, surface complexation, and electrostatic attraction mechanisms [17]. The adsorption process is governed by concentration gradients, contact time, pH, and the availability of active binding sites on the adsorbent surface. Activated carbon also effectively adsorbs dissolved organic compounds and  $\text{H}^+/\text{OH}^-$  ions, thereby contributing to pH adjustment toward neutral values [16].

The application of combined filtration and adsorption methods is expected to provide a more comprehensive and efficient treatment system through synergistic mechanisms [18]. In sequential configurations, filtration serves as a protective barrier that prevents premature clogging of downstream adsorption media by removing suspended solids and colloidal particles, thereby extending the operational lifespan and maintaining high adsorption efficiency [14]. Adsorption subsequently removes dissolved contaminants that escape physical filtration, ensuring comprehensive water quality improvement. Membrane filtration can be integrated as a final polishing stage to remove residual fine particles and provide an additional barrier against microbial contamination. Such multi-stage systems are particularly suitable for point-of-use applications in rural communities, as they utilize locally available materials (sand, activated carbon), operate without electricity through gravity-assisted flow or low-power pumps, and require minimal maintenance compared to chemical dosing systems [19]. However, limited field studies have systematically evaluated the performance of such combined systems under realistic tropical rainwater conditions, particularly regarding the optimization of media sequencing, determination of treatment kinetics, and assessment of long-term adsorption capacity.

This study aims to develop a practical and affordable point-of-use treatment system for rainwater harvesting to address clean water scarcity in Sungai Langka Village, Pesawaran Regency, Lampung Province. The specific objectives are: (1) to assess the rainwater harvesting quantity potential at the study location through hydrological analysis of 10-year rainfall data (2015–2024) using probability distribution meth-

ods and goodness-of-fit tests, with subsequent calculation of design rainfall intensity and potential harvested volume from rooftop catchment areas; (2) to optimize a three-stage sequential filtration-adsorption treatment system consisting of silica sand, activated carbon, and filter membrane by evaluating its performance boundaries under extreme contamination scenarios using artificial water samples with elevated pH (acidic and alkaline), TDS, and Fe concentrations; and (3) to evaluate the treatment performance with actual harvested rainwater by monitoring pH, TDS, and Fe removal efficiency over time, determining adsorption capacity, and assessing compliance with Indonesian Minister of Health Regulation No. 2/2023 standards for sanitary hygiene water (pH 6.5–8.5, TDS  $\leq 300$  mg/L, Fe  $\leq 0.3$  mg/L). This integrated assessment of both quantity potential and treatment quality is expected to provide a comprehensive framework for rainwater harvesting implementation in water-scarce rural communities.

## 2. Materials and Methods

### 2.1 Study Area

The research was conducted at the Center for Green and Sustainable Materials Laboratory, Institut Teknologi Sumatera, Lampung, Indonesia. Rainwater samples were collected from the Sungai Langka Village Hall, Pesawaran Regency, Lampung Province. The catchment area consisted of two roof types: galvanized iron (63.636  $\text{m}^2$ ) and asbestos (29.514  $\text{m}^2$ ), mapped using ArcGIS software.

### 2.2 Rainfall Data Analysis

Rainfall data from 2015–2024 was obtained from the Meteorology, Climatology, and Geophysics Agency (BMKG) of Pesawaran Regency, covering three rain gauge stations: Negeri Sakti, Kemiling, and Way Semah. Statistical analysis included calculation of mean, standard deviation, coefficient of variation ( $C_v$ ), coefficient of skewness ( $C_s$ ), and coefficient of kurtosis ( $C_k$ ).

Four probability distribution methods were evaluated: Normal, Log Normal, Gumbel, and Log Pearson Type III. Distribution selection was validated using Chi-Square and Smirnov-Kolmogorov tests. Rainfall intensity was calculated using the Mononobe method:

$$I = \frac{R_{24}}{24} \left( \frac{24}{t} \right)^{2/3} \quad (1)$$

where  $I$  is rainfall intensity (mm/hour),  $R_{24}$  is maximum 24-hour rainfall (mm), and  $t$  is rainfall duration (hours).

The time of concentration ( $T_c$ ) was calculated using the Kirpich formula, and potential harvested rainwater volume was estimated using the rational method:

$$Q = C \times I \times A \quad (2)$$

where  $Q$  is peak discharge ( $\text{m}^3/\text{hour}$ ),  $C$  is runoff coefficient,  $I$  is rainfall intensity (mm/hour), and  $A$  is catchment area ( $\text{m}^2$ ). Runoff coefficients of 0.9 and 0.8 were applied for galvanized iron and asbestos roofs, respectively.

### 2.3 Filtration-Adsorption System

The treatment system consisted of three filter columns in series, each containing a different media: silica sand, activated carbon, and filter membrane, respectively (Fig. 1). The three media were selected based on their complementary roles in water treatment [15, 16]. Silica sand served as the primary physical filtration medium, removing suspended

particles, sediment, and coarse contaminants through mechanical straining and sedimentation mechanisms. Activated carbon functioned as the adsorption medium, leveraging its highly microporous structure and large specific surface area to adsorb dissolved organic and inorganic pollutants, including heavy metal ions and compounds contributing to acidity and TDS. The filter membrane acted as the final polishing stage, removing fine colloidal particles and residual dissolved substances that passed through the preceding media.

Water was pumped from the inlet reservoir through the system via connecting pipes, passing through each media column sequentially before exiting through the outlet. The system was operated in a continuous-flow mode at a flow rate of approximately 1 L/min, with a total adsorbent media mass of 400 g distributed across the columns. This configuration maximized contact time between water and filter media to enhance contaminant removal efficiency.

Prior to use, silica sand and activated carbon underwent an activation process to remove residual contaminants and enhance adsorptive capacity. Silica sand was washed repeatedly with distilled water to eliminate fine dust and impurities, then oven-dried. Activated carbon was soaked in distilled water, washed to remove fine particles, and subsequently oven-dried to open and clear the adsorbent pores for optimal adsorption performance [15].

## 2.4 Artificial Water Testing

Prior to actual rainwater treatment, the system was optimized and its performance boundaries were evaluated using artificial water samples that simulated extreme rainwater contamination scenarios. This preliminary testing aimed to assess the maximum treatment capacity of each filter media under controlled conditions exceeding typical rainwater quality [5]. Four types of artificial water were prepared:

Acidic artificial water (initial pH 3.52) was prepared by adding dilute  $H_2SO_4$  to distilled water to simulate severe acid rain conditions caused by atmospheric  $SO_2$  and  $NO_x$  dissolution, while alkaline artificial water (initial pH 11.95) was prepared using NaOH solution to evaluate the system's capacity for pH reduction under highly alkaline conditions. High TDS artificial water (initial TDS 315 mg/L) was generated by dispersing clay powder in distilled water, exceeding the regulatory limit of 300 mg/L, to test the filtration efficiency for dissolved and suspended solids removal. Iron-containing artificial water (initial Fe 3.93 mg/L) was prepared by dissolving  $FeSO_4$  in distilled water, representing a concentration approximately 13 times the regulatory limit of 0.3 mg/L, to evaluate the adsorption capacity for heavy metal removal.

Each artificial water sample was processed through the treatment system under the same continuous-flow operating conditions. The deliberately extreme initial concentrations allowed characterization of the system's removal kinetics and identification of media saturation behavior prior to field deployment with actual rainwater samples.

## 2.5 Water Quality Analysis

Three key water quality parameters were selected for analysis: pH, total dissolved solids (TDS), and iron (Fe) concentration. These parameters were chosen based on their relevance to common rainwater quality issues in tropical regions, where atmospheric  $CO_2$  dissolution causes acidity, rooftop runoff introduces dissolved solids, and heavy metal contamination—particularly iron from galvanized roofing materials—poses health concerns [10, 11].

pH was measured using the electrometric method in accordance with SNI 06-6989.11-2004. A calibrated digital pH meter was used, with two-point calibration performed prior to each measurement session using standard buffer solutions at pH 4.01 and 7.01 to ensure instrument accuracy. TDS was determined following SNI 06-6989.27-2005 using a calibrated TDS meter. Iron (Fe) concentration was analyzed by UV-Vis spectrophotometry at a wavelength of 510 nm following SNI 06-6989.4-2009. In this method, Fe(II) ions react with 1,10-phenanthroline (orthophenanthroline) reagent in an acidic medium to form an orange-red complex, whose absorbance is proportional to the Fe concentration. A calibration curve was constructed using standard Fe solutions prior to sample analysis.

Water samples were collected from both the inlet and outlet of the treatment system at 15-minute intervals over a total treatment duration of 180 minutes. At each sampling point, the contaminant removal efficiency ( $\eta$ ) was calculated as:

$$\eta = \frac{C_{in} - C_{out}}{C_{in}} \times 100\% \quad (3)$$

where  $C_{in}$  and  $C_{out}$  are the influent and effluent concentrations (mg/L), respectively. Additionally, the adsorption capacity ( $q$ ) of the filter media for Fe removal was determined using:

$$q = \frac{(C_{in} - C_{out}) \times V}{m} \quad (4)$$

where  $V$  is the cumulative volume of treated water (L) and  $m$  is the total mass of adsorbent media (g). All treated water quality results were compared against the Indonesian Minister of Health Regulation No. 2/2023 standards for sanitary hygiene water: pH 6.5–8.5, TDS  $\leq$  300 mg/L, and Fe  $\leq$  0.3 mg/L.

## 3. Results and Discussion

### 3.1 Rainwater Harvesting Potential

Analysis of rainfall data from 2015–2024 revealed annual maximum rainfall ranging from 79 mm to 174.67 mm (Table 1). The average annual maximum rainfall from each of the three rain gauge stations—Negeri Sakti, Kemiling, and Way Semah—was calculated to represent the spatial distribution of rainfall across Pesawaran Regency. The highest average occurred in 2017 (174.67 mm), primarily driven by an exceptionally high reading at Way Semah station (292 mm), while the lowest was recorded in 2023 (79 mm).

**Table 1.** Maximum annual rainfall in Pesawaran Regency (2015–2024)

Year	Negeri Sakti (mm)	Kemiling (mm)	Way Semah (mm)	Avg. (mm)
2015	75	75	107	85.67
2016	77	102	108	95.67
2017	92	140	292	174.67
2018	97	76	98	90.33
2019	139	130	85	118.00
2020	80	125	97	100.67
2021	77	91	76	81.33
2022	68	112	71	83.67
2023	88	56	93	79.00
2024	114	150	126	130.00

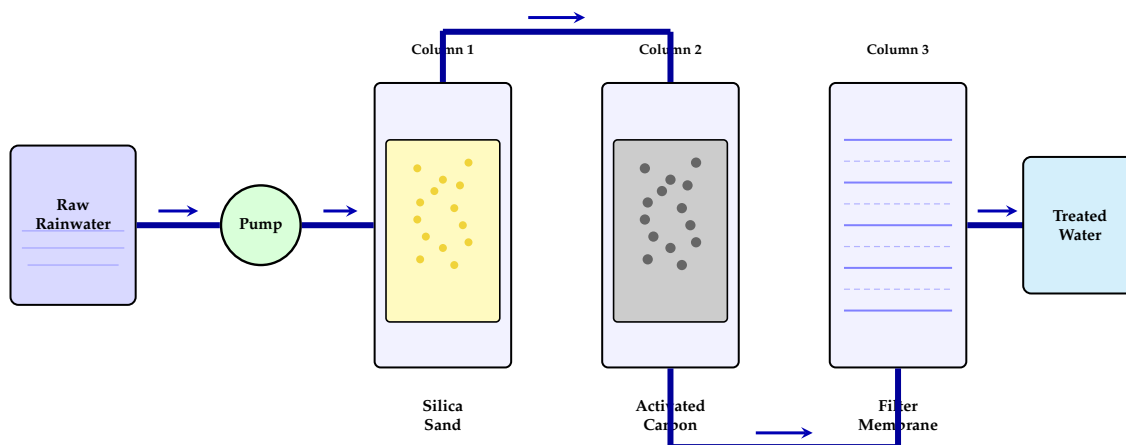


**Figure 1.** Schematic illustration of the filtration-adsorption reactor system consisting of three sequential columns: silica sand, activated carbon, and filter membrane.

Descriptive statistical analysis of the averaged rainfall data yielded a mean of 103.9 mm, standard deviation of 29.85, coefficient of variation ( $C_v$ ) of 0.29, coefficient of skewness ( $C_s$ ) of 1.73, and coefficient of kurtosis ( $C_k$ ) of 6.63. These statistical parameters were used to evaluate the suitability of four probability distribution methods: Gumbel, Normal, Log Normal, and Log Pearson Type III. The positive skewness ( $C_s = 1.73$ ) indicated a right-skewed distribution, suggesting that extreme rainfall events occur occasionally but with considerable magnitude.

All four distributions were subsequently validated using the Smirnov-Kolmogorov and Chi-Square goodness-of-fit tests (Table 2). The Smirnov-Kolmogorov test accepted all four distributions at the 5% significance level, as the computed statistics (0.13–0.18) were below the critical value of 0.41. However, the Chi-Square test provided a more discriminating result: only the Gumbel ( $\chi^2 = 3$ ) and Normal ( $\chi^2 = 5$ ) distributions passed the critical threshold of 5.991, while the Log Normal and Log Pearson Type III distributions ( $\chi^2 = 7$  each) were rejected. Since the Gumbel distribution yielded the lowest Chi-Square value and is widely recommended for extreme rainfall analysis in hydrology [2, 20], it was selected for subsequent design rainfall calculations.

Using the Gumbel distribution, design rainfall values were calculated for multiple return periods (Table 3). For a 2-year return period, the design rainfall was 99.86 mm, while the 100-year return period yielded 232.94 mm. The increasing design rainfall with longer return periods reflects the higher probability of extreme rainfall events occurring over extended time horizons.

The time of concentration ( $T_c$ ) was calculated using the Kirpich formula for three roof sections with varying heights and flow path lengths. The maximum  $T_c$  value of 8.81 minutes was adopted for analysis, representing the longest travel time for flow to reach the control point and thereby anticipating the worst-case scenario for drainage capacity design. Using this  $T_c$  value and the 2-year return period design rainfall (99.86 mm) in the Mononobe equation, the rainfall intensity was determined to be 124.38 mm/hour. This 2-year return period was selected as it represents the most frequent rainfall condition relevant to the operational lifespan of the treatment system.

The potential harvested rainwater volume was subsequently estimated using the rational method (Table 4). The

galvanized iron roof ( $C = 0.9$ ,  $A = 63.636 \text{ m}^2$ ) yielded a discharge of  $7.12 \text{ m}^3/\text{hour}$ , while the asbestos roof ( $C = 0.8$ ,  $A = 29.514 \text{ m}^2$ ) yielded  $2.94 \text{ m}^3/\text{hour}$ . The higher harvesting potential of the galvanized iron roof is attributed to both its larger catchment area and higher runoff coefficient, as metallic surfaces exhibit lower water retention compared to fibrous asbestos materials [21]. These results demonstrate that roof material type and catchment area size are critical factors influencing rainwater harvesting potential, and provide essential information for determining the capacity of storage and treatment systems.

## 3.2 System Optimization with Artificial Water

### 3.2.1 pH Treatment Performance

For acidic artificial water (initial pH 3.52), the treatment system increased pH to 5.34 after 180 minutes of treatment (Fig. 2a). The pH adjustment exhibited a characteristic two-phase kinetic pattern: a rapid neutralization phase during the first 90 minutes, followed by a slower equilibrium phase. This behavior can be attributed to the sequential contribution of each filter media. Silica sand, whose surface contains silanol groups ( $\text{Si-OH}$ ), facilitated partial neutralization through proton exchange with  $\text{H}^+$  ions in the acidic solution [13]. Activated carbon contributed further via adsorption of  $\text{H}^+$  onto its negatively charged surface groups (e.g., carboxyl, hydroxyl, carbonyl) and ion exchange [15, 17]. The gradual decrease in neutralization rate after 90 minutes reflected progressive saturation of the available active sites on both media surfaces.

For alkaline artificial water (initial pH 11.95), pH decreased to 11.10 after 180 minutes (Fig. 2a). The most significant reduction occurred within the first 60 minutes, primarily driven by the adsorption of  $\text{OH}^-$  ions onto the positively charged sites of activated carbon under alkaline conditions. However, the relatively modest overall pH reduction ( $\Delta\text{pH} = 0.85$ ) compared to the acidic treatment ( $\Delta\text{pH} = 1.82$ ) suggests that the filter media exhibited a stronger affinity for  $\text{H}^+$  adsorption than for  $\text{OH}^-$  removal. This asymmetry is consistent with the predominantly negative surface charge of both silica sand and activated carbon at elevated pH, which creates electrostatic repulsion with  $\text{OH}^-$  anions and limits adsorption efficiency [16]. The final pH remaining well above neutral (7.0) indicates that the system's alkaline buffering capacity was limited under these extreme conditions, though

**Table 2.** Goodness-of-fit test results for probability distribution selection

Test	Gumbel	Normal	Log Normal	Log Pearson III
<i>Smirnov-Kolmogorov (critical value = 0.41)</i>				
Computed value	0.13	0.18	0.14	0.15
Result	Accepted	Accepted	Accepted	Accepted
<i>Chi-Square (critical value = 5.991)</i>				
Computed value	3	5	7	7
Result	Accepted	Accepted	Rejected	Rejected

**Table 3.** Design rainfall for various return periods using the Gumbel distribution

Return period (year)	$Y_{Tr}$	$K_{Tr}$	$X_{Tr}$ (mm)
2	0.367	-0.136	99.86
5	1.500	1.058	135.48
10	2.250	1.848	159.07
25	3.199	2.847	188.88
50	3.902	3.587	210.99
100	4.600	4.322	232.94

such highly alkaline rainwater is uncommon in tropical environments.

**3.2.2 TDS Removal**

Initial TDS of 315 mg/L decreased to 118 mg/L after 150 minutes, achieving a removal efficiency of 62.54% (Fig. 2b). The removal kinetics followed a two-phase pattern: a rapid initial reduction within the first 75 minutes, followed by a plateau phase where efficiency stabilized. During the initial phase, TDS removal was driven by the synergistic action of all three media. Silica sand physically trapped suspended clay particles through mechanical straining and depth filtration, while activated carbon adsorbed dissolved organic and inorganic solutes through van der Waals forces and electrostatic interactions on its microporous surface [15]. The filter membrane provided an additional polishing step by rejecting fine colloidal particles that passed through the preceding media.

The transition to the plateau phase after 75 minutes indicated progressive saturation of the adsorption sites on the activated carbon surface, which reduced the driving force for further mass transfer from the liquid phase to the solid adsorbent [16]. Despite the reduced rate, the final TDS concentration of 118 mg/L was well below the regulatory limit of 300 mg/L, demonstrating adequate treatment capacity even under the deliberately elevated initial loading condition. The 62.54% removal efficiency achieved with artificial water provided a baseline for predicting system performance with actual rainwater, which typically exhibits substantially lower TDS levels.

**3.2.3 Iron (Fe) Removal**

Initial Fe concentration of 3.93 mg/L decreased to 0.70 mg/L after 180 minutes, corresponding to an overall removal efficiency of 82.19% (Fig. 2c). The removal kinetics exhibited a rapid initial phase during the first 30 minutes, with concentration dropping sharply to 0.63 mg/L. This rapid removal can be attributed to the abundance of unoccupied adsorption sites and the large concentration gradient between the

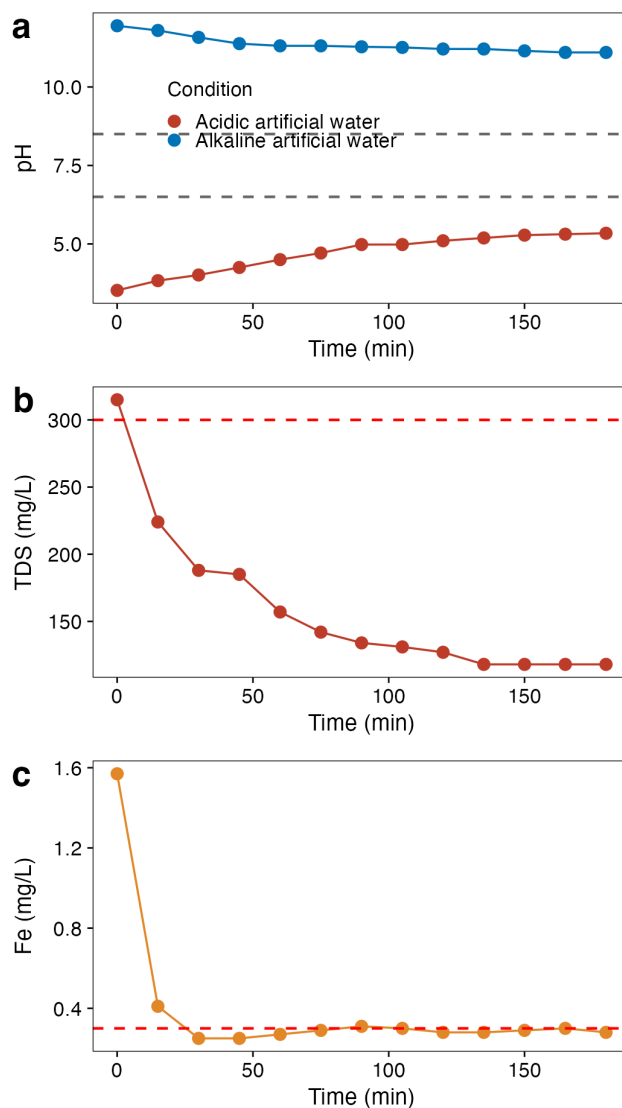


**Figure 2.** System optimization with artificial water: (a) pH for acidic and alkaline conditions, (b) TDS reduction, (c) Fe removal over 180 min. Dashed lines indicate regulatory limits.

solution and the adsorbent surface, which provided a strong driving force for mass transfer [15].

Following the initial rapid phase, the Fe concentration fluctuated within the range of 0.63–0.77 mg/L, indicating that the system was approaching dynamic adsorption equilibrium. These fluctuations are characteristic of competitive

**Table 4.** Potential harvested rainwater volume by roof type

Roof type	C	I (mm/h)	A (m <sup>2</sup> )	Q (L/h)	Q (m <sup>3</sup> /h)
Galvanized iron	0.9	124.38	63.636	7123.48	7.12
Asbestos	0.8	124.38	29.514	2936.74	2.94

adsorption processes, where previously adsorbed Fe ions may be partially displaced by other species or released due to localized pH changes at the adsorbent surface [16]. The primary removal mechanisms involved physical filtration of Fe-containing suspended particles by silica sand, followed by adsorption of dissolved Fe(II) and Fe(III) ions onto activated carbon through a combination of surface complexation, ion exchange, and electrostatic attraction. Activated carbon’s highly developed microporous structure, with specific surface areas typically ranging from several hundreds to over a thousand m<sup>2</sup>/g, provided abundant active sites for Fe ion retention [18].

Although the final Fe concentration of 0.70 mg/L exceeded the regulatory limit of 0.3 mg/L under this extreme loading condition (3.93 mg/L, approximately 13 times the standard), the high removal percentage demonstrated the system’s strong affinity for Fe adsorption, suggesting that effective compliance could be achieved with the lower Fe concentrations typically found in actual rainwater.

**3.3 Rainwater Treatment Performance**

Following the system optimization with artificial water, the treatment system was applied to actual rainwater samples collected from the rooftop catchment area at Sungai Langka Village Hall. Unlike the deliberately extreme conditions used in the artificial water tests, the actual rainwater represented realistic field conditions with moderate contamination levels. The treatment performance was evaluated over a 180-minute period for the same three parameters—pH, TDS, and Fe—to assess whether the system could bring the harvested rainwater into compliance with the Indonesian Minister of Health Regulation No. 2/2023 standards for sanitary hygiene water (Fig. 3).

**3.3.1 pH Enhancement**

Rainwater pH increased from 6.83 to 7.65 over 180 min of treatment (Fig. 3a), shifting from slightly acidic to near-neutral. The initial pH of 6.83 is typical of tropical rainwater, where dissolved CO<sub>2</sub> forms carbonic acid (H<sub>2</sub>CO<sub>3</sub>) and trace SO<sub>2</sub>/NO<sub>x</sub> add acidity [6, 7]. In contrast to the extreme conditions of the artificial water test (pH 3.52), the relatively mild acidity of actual rainwater allowed the treatment system to achieve effective neutralization well within the regulatory range.

The pH adjustment progressed gradually throughout the 180-minute treatment period, with each media contributing through distinct mechanisms. Silica sand physically removed acidic suspended particles and partially neutralized H<sup>+</sup> ions through surface silanol group interactions [13]. Activated carbon further adsorbed residual H<sup>+</sup> ions and dissolved weak acid species (e.g., dissolved CO<sub>2</sub> and organic acids) via its surface functional groups. The filter membrane contributed to pH stabilization by removing fine acidic colloidal particles that could otherwise buffer the solution at lower pH values. The final pH of 7.65 comfortably met the regulatory standard of 6.5–8.5, indicating that the combined system is well-suited

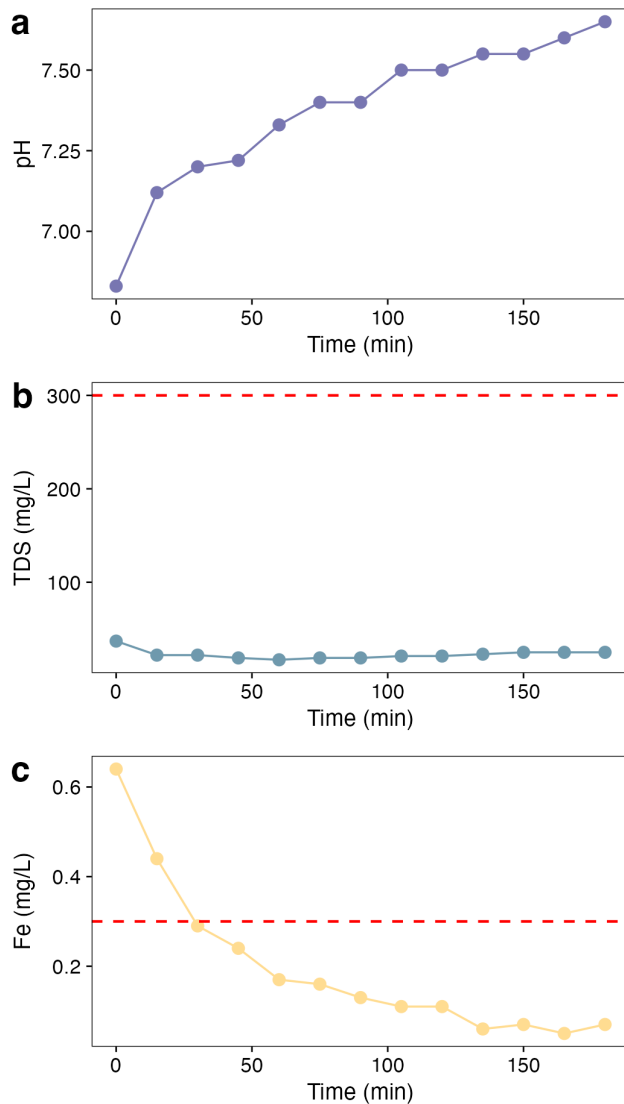


**Figure 3.** Rainwater treatment: (a) pH into regulatory range 6.5–8.5, (b) TDS vs. 300 mg/L limit, (c) Fe vs. 0.3 mg/L standard.

for neutralizing the mild acidity typical of harvested rainwater in tropical environments.

**3.3.2 TDS Reduction**

Rainwater TDS decreased from 37 mg/L to a minimum of 17 mg/L at 60 minutes, then stabilized around 22–25 mg/L for the remainder of the treatment period (Fig. 3b). The peak removal efficiency of 54% achieved at 60 minutes is noteworthy considering the already low initial TDS concentration, which was well below the regulatory limit of 300 mg/L even before treatment.

The TDS removal kinetics followed a pattern consistent

with the artificial water test, exhibiting a rapid initial decline followed by stabilization. During the first 60 minutes, the high availability of unoccupied adsorption sites on activated carbon and clean interstices within the silica sand bed facilitated efficient removal of dissolved and suspended solids [15]. The slight TDS increase from 17 to 22–25 mg/L after 60 min can be attributed to partial desorption of weakly bound solutes as the media approached equilibrium, as often seen in continuous-flow adsorption [16]. Despite this minor rebound, all post-treatment TDS values remained substantially below the 300 mg/L standard, with a margin exceeding 90%. The relatively low initial TDS of actual rainwater (37 mg/L), compared to the artificial water test (315 mg/L), confirms that the treatment system operates well within its capacity under realistic field conditions.

### 3.3.3 Iron (Fe) Removal

Fe concentration decreased dramatically from 0.64 mg/L to 0.07 mg/L after 165 minutes, achieving an overall removal efficiency of 89.06% (Fig. 3c). The initial Fe concentration of 0.64 mg/L, which exceeded the regulatory limit of 0.3 mg/L, is attributed to the leaching of iron from galvanized roofing materials during rainwater collection [10–12]. This finding underscores the necessity of post-collection treatment for rooftop-harvested rainwater.

The Fe removal kinetics exhibited a characteristic rapid decline within the first 60 minutes (0.64 to 0.17 mg/L), followed by a gradual approach to the final equilibrium concentration. This two-phase behavior is consistent with adsorption theory: the initial rapid removal reflects abundant available binding sites and a large concentration gradient driving mass transfer, while the subsequent slower phase results from decreasing site availability and diminishing driving force as the system approaches equilibrium [15]. Each media contributed sequentially to Fe removal. Silica sand served as the primary physical filter, trapping Fe-containing suspended particles and Fe(OH)<sub>3</sub> precipitates formed through natural oxidation of dissolved Fe(II) to Fe(III) [22, 23]. Activated carbon subsequently adsorbed residual dissolved Fe(II) and Fe(III) ions through surface complexation with oxygen-containing functional groups, ion exchange, and electrostatic attraction within its microporous structure [18, 17]. The filter membrane provided final polishing by rejecting residual fine particles and colloidal iron species.

The adsorption capacity increased progressively from 0 to 0.252 mg/g over 180 minutes (Table 5), with no indication of reaching a plateau. This continuously increasing trend suggests that the adsorbent media had not yet reached saturation, implying that the system retains additional capacity for prolonged operation beyond the 180-minute test period. The final Fe concentration of 0.07 mg/L was well below the regulatory limit of 0.3 mg/L, representing a safety margin of approximately 77%. Compared to the artificial water test, where the system could not reduce Fe below 0.70 mg/L from an initial concentration of 3.93 mg/L, the successful compliance achieved with actual rainwater (initial Fe 0.64 mg/L) validates the artificial water testing approach as a conservative performance predictor.

### 3.4 Compliance with Water Quality Standards

Table 6 summarizes the comparison between the initial and final quality of treated rainwater against the Indonesian Minister of Health Regulation No. 2/2023 standards for sanitary hygiene water. All three monitored parameters achieved full

**Table 5.** Fe adsorption efficiency in rainwater treatment

Time (min)	C <sub>in</sub> (mg/L)	C <sub>out</sub> (mg/L)	ΔFe (mg/L)	Vol. (L)	Eff. (mg/g)
0	0.64	0.64	0.00	0	0.000
30	0.64	0.29	0.35	30	0.026
60	0.64	0.17	0.46	60	0.069
90	0.64	0.13	0.51	90	0.114
120	0.64	0.11	0.53	120	0.157
150	0.64	0.07	0.56	150	0.210
180	0.64	0.07	0.56	180	0.252

compliance after treatment, confirming the effectiveness of the combined filtration-adsorption system.

Among the three parameters, iron removal demonstrated the most critical improvement. The initial Fe concentration of 0.64 mg/L exceeded the regulatory limit of 0.3 mg/L, posing a direct non-compliance risk if rainwater were used without treatment. After treatment, the Fe concentration decreased to 0.07 mg/L, representing a 77% safety margin below the standard. The pH was adjusted from slightly acidic (6.83) to near-neutral (7.65), placing it comfortably within the 6.5–8.5 range. Although the initial TDS of 37 mg/L was already well below the 300 mg/L limit, the treatment further reduced it to 22 mg/L with a 40.54% removal efficiency, indicating the system's capacity to handle higher TDS loads if necessary.

These results are comparable to or better than those reported in other rainwater treatment studies. Duran-Romero et al. [13] reported effective removal of suspended solids using biosand filtration, though without the adsorption stage that enhances dissolved contaminant removal. Morales-Figueroa et al. [5] demonstrated similar multi-stage treatment approaches for rainwater, achieving compliance with local standards. The present system offers a practical advantage through the use of locally available, low-cost materials (silica sand and activated carbon) in a simple gravity- and pump-driven configuration, without chemical dosing or electricity-intensive processes.

From a practical standpoint, the full compliance of all parameters confirms that the combined filtration-adsorption system is suitable for deployment as a point-of-use treatment solution for rainwater harvesting in water-scarce rural communities such as Sungai Langka Village [19, 14]. The system transforms non-compliant rainwater (particularly with respect to Fe) into water that meets sanitary hygiene standards for domestic non-potable uses including bathing, washing, and general household cleaning [4, 9].

## 4. Conclusions

This study successfully demonstrated the effectiveness of combined filtration and adsorption using silica sand, activated carbon, and filter membrane for rainwater treatment. Rainwater harvesting potential in Sungai Langka Village was determined as 7.12 m<sup>3</sup>/hour for galvanized iron roofs (C = 0.9) and 2.94 m<sup>3</sup>/hour for asbestos roofs (C = 0.8), based on 10-year rainfall data analysis using the Gumbel distribution method. The combined filtration-adsorption system showed high effectiveness in removing contaminants from both artificial and actual rainwater samples, successfully shifting acidic and alkaline pH toward neutral values and significantly reducing TDS and Fe concentrations. Treated rainwater quality met all Indonesian Minister of Health Regulation

**Table 6.** Treated rainwater quality compared to regulatory standards

Parameter	Before	After	Removal	Standard	Status
pH	6.83	7.65	—	6.5–8.5	Compliant
TDS (mg/L)	37	22	40.54%	≤ 300	Compliant
Fe (mg/L)	0.64	0.07	89.06%	≤ 0.3	Compliant

No. 2/2023 standards: pH improved from 6.83 to 7.65 (standard: 6.5–8.5), TDS decreased from 37 to 22 mg/L (standard: ≤ 300 mg/L), and Fe reduced from 0.64 to 0.07 mg/L (standard: ≤ 0.3 mg/L). The developed system offers a practical and affordable solution for improving clean water access in water-scarce rural communities. Future work should focus on scaling up the system for household or community-level implementation, establishing maintenance schedules for media replacement, and incorporating additional parameters such as microbiological testing.

### Acknowledgments

The authors thank the Meteorology, Climatology, and Geophysics Agency (BMKG) of Lampung Province for providing rainfall data, and the Center for Green and Sustainable Materials Laboratory, Institut Teknologi Sumatera for research facilities.

### REFERENCES

- [1] H. Hasibuan, B. Elizandri, F. Asrofani, G. Putra, Potential application of rain water harvesting technology as an alternative clean water source to mitigate land subsidence, *Global J. Environ. Sci. Manage.* 11 (1) (Jan. 2025). <https://doi.org/10.22034/gjesm.2025.01.17>.
- [2] A. Raimondi, R. Quinn, G. R. Abhijith, G. Becciu, A. Ostfeld, Rainwater Harvesting and Treatment: State of the Art and Perspectives, *Water* 15 (8) (2023) 1518. <https://doi.org/10.3390/w15081518>.
- [3] A. Raimondi, R. Quinn, I. Gnecco, A. Ostfeld, New Advances in Rainwater Harvesting and Treatment, *Water* 16 (11) (2024) 1591. <https://doi.org/10.3390/w16111591>.
- [4] A. M. Rodrigues, K. T. M. Formiga, J. Milograna, Integrated systems for rainwater harvesting and greywater reuse: A systematic review of urban water management strategies, *Water Supply* 23 (10) (2023) 4112–4125. <https://doi.org/10.2166/ws.2023.240>.
- [5] C. Morales-Figueroa, L. A. Castillo-Suárez, I. Linares-Hernández, V. Martínez-Miranda, E. A. Teutli-Sequeira, Treatment processes and analysis of rainwater quality for human use and consumption regulations, treatment systems and quality of rainwater, *Int. J. Environ. Sci. Technol.* 20 (8) (2023) 9369–9392. <https://doi.org/10.1007/s13762-023-04802-2>.
- [6] Z. Gao, Q. Zhang, Y. Wang, X. Jv, M. Dzakpasu, X. C. Wang, Evolution of water quality in rainwater harvesting systems during long-term storage in non-rainy seasons, *Science of The Total Environment* 912 (2024) 168784. <https://doi.org/10.1016/j.scitotenv.2023.168784>.
- [7] C. Payus, C. Jikilim, J. Sentian, Rainwater chemistry of acid precipitation occurrences due to long-range transboundary haze pollution and prolonged drought events during southwest monsoon season: Climate change driven, *Heliyon* 6 (9) (2020) e04997. <https://doi.org/10.1016/j.heliyon.2020.e04997>.
- [8] J. K. Maykot, I. C. Martins Vaz, E. Ghisi, Characterisation of First Flush for Rainwater Harvesting Purposes in Buildings, *Water* 17 (12) (2025) 1772. <https://doi.org/10.3390/w17121772>.
- [9] J. J. Lay, J. R. Vogel, J. B. Belden, G. O. Brown, D. E. Storm, Water Quality and the First-Flush Effect in Roof-Based Rainwater Harvesting, Part II: First Flush, *Water* 16 (10) (2024) 1421. <https://doi.org/10.3390/w16101421>.
- [10] I. H. Igbinoso, I. T. Aighewi, Assessment of the Physicochemical and Heavy Metal Qualities of Rooftop Harvested Rainwater in a Rural Community, *Global Challenges* 1 (6) (2017) 1700011. <https://doi.org/10.1002/gch2.201700011>.
- [11] F. Anabtawi, N. Mahmoud, I. A. Al-Khatib, Y.-T. Hung, Heavy Metals in Harvested Rainwater Used for Domestic Purposes in Rural Areas: Yatta Area, Palestine as a Case Study, *IJERPH* 19 (5) (2022) 2683. <https://doi.org/10.3390/ijerph19052683>.
- [12] B. M. Tengan, O. Akoto, Comprehensive evaluation of the possible impact of roofing materials on the quality of harvested rainwater for human consumption, *Science of The Total Environment* 819 (2022) 152966. <https://doi.org/10.1016/j.scitotenv.2022.152966>.
- [13] D. A. Duran Romero, M. C. De Almeida Silva, B. J. M. Chaúque, A. D. Benetti, Biosand Filter as a Point-of-Use Water Treatment Technology: Influence of Turbidity on Microorganism Removal Efficiency, *Water* 12 (8) (2020) 2302. <https://doi.org/10.3390/w12082302>.
- [14] R. Shaheed, W. H. M. Wan Mohtar, A. El-Shafie, Ensuring water security by utilizing roof-harvested rainwater and lake water treated with a low-cost integrated adsorption-filtration system, *Water Science and Engineering* 10 (2) (2017) 115–124. <https://doi.org/10.1016/j.wse.2017.05.002>.
- [15] H. N. Tran, Adsorption Technology for Water and Wastewater Treatments, *Water* 15 (15) (2023) 2857. <https://doi.org/10.3390/w15152857>.
- [16] I. Pet, M. N. Sanad, M. Farouz, M. M. ElFaham, A. El-Hussein, M. S. A. El-sadek, R. A. Althobiti, A. Ioanid, Review: Recent Developments in the Implementation of Activated Carbon as Heavy Metal Removal Management, *Water Conserv Sci Eng* 9 (2) (2024) 62. <https://doi.org/10.1007/s41101-024-00287-3>.
- [17] X. Yang, Y. Wan, Y. Zheng, F. He, Z. Yu, J. Huang, H. Wang, Y. S. Ok, Y. Jiang, B. Gao, Surface functional groups of carbon-based adsorbents and their roles in the removal of heavy metals from aqueous solutions: A critical review, *Chemical Engineering Journal* 366 (2019) 608–621. <https://doi.org/10.1016/j.cej.2019.02.119>.
- [18] S. Y. Yoon, H. Kim, R. Valiyaveetil Basheer, N. Abd Rahman, S. B. Jang, K. T. Wong, D. H. Moon, C. E. Choong, M. Jang, Mg/Si- and Ag-Doped Carbon-Based Media Rainwater Filtration System for Multiple Pollutants Removal, *Materials* 17 (22) (2024) 5638. <https://doi.org/10.3390/ma17225638>.
- [19] C. K. Pooi, H. Y. Ng, Review of low-cost point-of-use water treatment systems for developing communities, *npj Clean Water* 1 (1) (2018) 11. <https://doi.org/10.1038/s41545-018-0011-0>.
- [20] C. G. Anghel, Revisiting the Use of the Gumbel Distribution: A Comprehensive Statistical Analysis Regarding Modeling Extremes and Rare Events, *Mathematics* 12 (16) (2024) 2466. <https://doi.org/10.3390/math12162466>.
- [21] R. Farreny, T. Morales-Pinzón, A. Guisasaola, C. Tayà, J. Rieradevall, X. Gabarrell, Roof selection for rainwater harvesting: Quantity and quality assessments in Spain, *Water Research* 45 (10) (2011) 3245–3254. <https://doi.org/10.1016/j.watres.2011.03.036>.
- [22] D. Vries, C. Bertelkamp, F. Schoonenberg Kegel, B. Hofs, J. Dusseldorp, J. Bruins, W. De Vet, B. Van Den Akker, Iron and manganese removal: Recent advances in modelling treatment efficiency by rapid sand filtration, *Water Research* 109 (2017) 35–45. <https://doi.org/10.1016/j.watres.2016.11.032>.
- [23] S. Chaturvedi, P. N. Dave, Removal of iron for safe drinking water, *Desalination* 303 (2012) 1–11. <https://doi.org/10.1016/j.desal.2012.07.003>.